Plasmon Injection to Compensate and Control Losses in Negative Index Metamaterials

Mehdi Sadatgol,[1] Şahin K. Özdemir,[2] Lan Yang,[2] and Durdu Ö. Güney[1,*]
[1]Department of Electrical and Computer Engineering, Michigan Technological University, Houghton, Michigan 49931, USA
[2]Department of Electrical and Systems Engineering, Washington University, St. Louis, Missouri 63130, USA
(Received 2 June 2014; published 16 July 2015)

Metamaterials have introduced a whole new world of unusual materials with functionalities that cannot be attained in naturally occurring material systems by mimicking and controlling the natural phenomena at subwavelength scales. However, the inherent absorption losses pose a fundamental challenge to the most fascinating applications of metamaterials. Based on a novel plasmon injection (PI or Π) scheme, we propose a coherent optical amplification technique to compensate losses in metamaterials. Although the proof of concept device here operates under normal incidence only, our proposed scheme can be generalized to an arbitrary form of incident waves. The Π scheme is fundamentally different from major optical amplification schemes. It does not require a gain medium, interaction with phonons, or any nonlinear medium. The Π scheme allows for loss-free metamaterials. It is ideally suited for mitigating losses in metamaterials operating in the visible spectrum and is scalable to other optical frequencies. These findings open the possibility of reviving the early dreams of making "magical" metamaterials from scratch.

DOI: 10.1103/PhysRevLett.115.035502 PACS numbers: 81.05.Xj, 73.20.Mf, 78.67.Pt

Metamaterials have led to previously unthought of applications such as a flat lens [1], perfect lens [2], hyperlens [3–5], ultimate illusion optics [6–8], perfect absorber [9,10], optical analog simulators [11,12], meta-spacers [13], and many others. Despite tremendous progress in theory and experimental realizations, the major current challenges seem to further delay the metamaterial era to come. For instance, achieving full isotropy, feasible fabrication methods, broad bandwidth, and compensation of dissipative losses especially at optical frequencies are among the challenges yet to be solved [14,15]. Perhaps the most critical of all is how to avoid optical losses—especially in large-volume structures. The performance of devices utilizing metamaterials dramatically degrades at optical frequencies due to significant Ohmic losses arising from the metallic constituents. The strategies proposed to mitigate the losses include passive reduction and active compensation schemes. Avoiding sharp edges [16], reducing skin depths [16–18], and classical analog of electromagnetically induced transparency are proposed as passive loss minimization techniques [19,20]. Constitutive materials such as dielectrics [21], nitrides [22], oxides [23], graphene [24], and superconductors [24–30] have also been explored for possible alternatives to lossy conductors. However, so far none of these materials has been shown to outperform the performance of high-conductivity metals at room temperature [31,32]. Active compensation of losses using a gain medium has emerged as the most promising strategy to avoid the deleterious impacts of losses on metamaterial devices. Optically pumped semiconductor quantum dots and quantum wells incorporated in planar metamaterials have been experimentally shown to compensate the losses to some extent [33–38]. A remarkable improvement in the figure of merit (FOM) of a negative refractive index of a fishnet metamaterial operating in the visible range has been recorded using dye molecules embedded in epoxy resin and pumped by picosecond pulses [35,37]. Although important progress has been made in theory [14,15,34,35,38–40] and experiments [14,15,33,36,37,41–43], there still exist concerns about the viability of active compensation of loss by gain medium for practically large-volume metamaterials [14]. First, it was shown that causality and the stability of the system make the loss compensation difficult without compromising interesting properties of the metamaterials [14,44,45]. Second, the requirement for optical or electrical pumping makes the metamaterials complex and dependent on available pump sources or gain materials at particular wavelengths. Third, high maintenance and the short chemical life of the dye molecules make the durable metamaterials unfeasible [35,37].

Here, we propose a novel optical amplification technique to compensate and control losses in metamaterials. Our proposed amplification scheme is ideally suited for compensating losses in metamaterials operating in the visible spectrum and is fundamentally different from major amplification schemes based on stimulated optical emission, Raman scattering, and optical parametric amplification, or recently proposed surface plasmon polariton (SPP) amplification for plasmonic integrated circuits [43]. It does not require gain medium, interaction with phonons, or any nonlinear medium, and it operates at room temperature. Our technique relies on the constructive interference of externally injected SPPs within the metamaterial to coherently amplify the domestic SPPs of the metamaterial. The amplified SPPs are then coupled into the free space via an

appropriately designed grating network at the output port of the metamaterial. In this Letter, we show that this proposed scheme, referred to as the Π scheme, provides diverging FOM, hence, loss-free optical metamaterials without using an optical gain providing medium. Although the negative index metamaterial (NIM) described here is functional for normally incident plane waves only, the Π scheme can be generalized to an arbitrary form of incident waves.

Below, we first describe how the Π scheme improves the FOM of NIMs based on a conceptual plasmonic structure. Then, we examine the simulations and effective parameter retrieval results [46–49] to characterize and validate the improved performance offered by the proposed scheme.

Figure 1 illustrates the conceptual structure that is built by arranging the unit cell of a so-called "surface plasmon driven (SPD) NIM" [49,50] into three superlattices. Each superlattice is built by repeating the unit cell, indicated by the red rectangular box, an integer number of times except that the superlattices at the sides have missing grating above the thin film. This prevents the coupling of SPPs back to free-space photons, because the gratings are designed to facilitate the coupling between the photons and the SPPs. The central superlattice is intended as the metamaterial where the losses are to be compensated. As shown in Fig. 1, the SPPs that are excited by the auxiliary ports, P_3 and P_4, at the side superlattices propagate toward the central superlattice to form a standing wave. Then these SPPs injected from the side superlattices to the central superlattice amplify the domestic SPPs excited by the input port P_1 (i.e., no input field at P_1 is supplied in Fig. 1 to clearly show injected SPPs only). We design the structure such that all of these three SPP waves interfere constructively at the central superlattice. The amplified SPPs are finally converted back to the free-space photons at the output port P_2 facilitated by the grating above the thin film in the central superlattice. A detailed working principle and general theory of the proposed loss compensation scheme and amplification are given in Ref. [51].

We performed frequency domain analysis of the structure using the finite element method in COMSOL MULTIPHYSICS to find the multiport scattering parameters. The Drude model with plasma frequency $f_p = 2175$ THz and collision frequency $f_c = 6.5$ THz was used to describe gold [16]. Polyimide layers have relative permittivity $\varepsilon_r = 3.6$. Since the ports P_3 and P_4 of the structure in Fig. 1 are the auxiliary ports to compensate the dissipated power, the structure in Fig. 1 can be effectively modeled as a one-input–one-output structure with P_1 and P_2 being the actual input and output ports, respectively, for the metamaterial (i.e., central superlattice). Thus, having in hand the scattering parameters from COMSOL simulation, we calculated the effective refractive index and the wave impedance of our plasmonic structure using the retrieval procedure [17,47–49,58–62], which includes equations based on the transformation matrix of a one-input–one-output homogeneous slab. Then the overall scattering parameters of our central superlattice are given as [51]

$$S_{11} = S'_{11} + \sqrt{\alpha/2}(S'_{13} + S'_{14}), \tag{1a}$$

$$S_{21} = S'_{21} + \sqrt{\alpha/2}(S'_{23} + S'_{24}), \tag{1b}$$

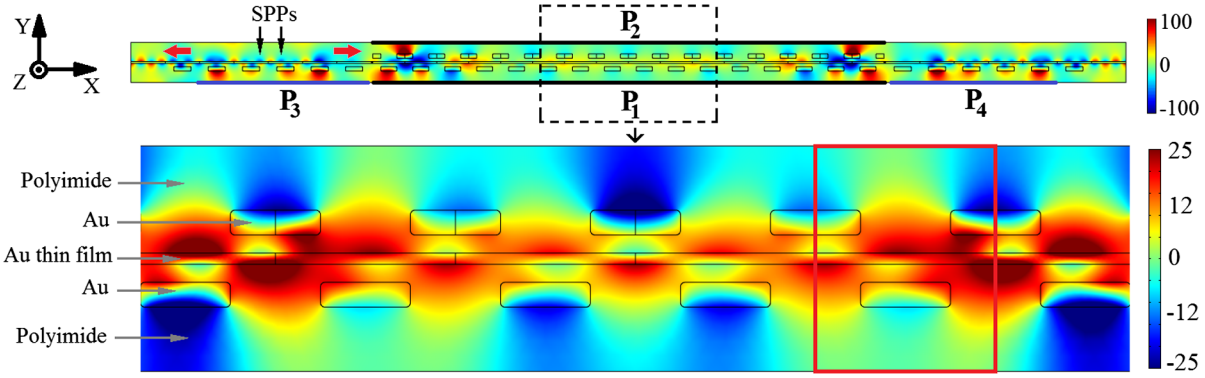

FIG. 1 (color online). Conceptual structure for the Π scheme. The central superlattice constitutes the metamaterial. P_1 and P_2 are the input and output ports of the metamaterial, respectively. P_3 and P_4 are the auxiliary ports through which surface plasmons for amplification are excited externally. The red rectangular box illustrates the metamaterial unit cell consisting of gold grating and the gold thin film (in the center of the unit cell) embedded in polyimide. The thickness of the gold thin film and its distance from the strips are 5 and 8 nm, respectively. The thickness of the gold strips in the gratings is 11 nm. Grating period at the central superlattice (i.e., between the ports P_1 and P_2) is 80 and 86 nm at the side superlattices above the ports P_3 and P_4. There exist six periods in each of the side superlattices and 16 periods in the central superlattice. The structure is translationally invariant in the z direction. SPPs propagate from the side superlattices to central superlattice and excite the metamaterial eigenmode (lower panel), which in turn amplifies the domestic SPPs in the central superlattice if an input field at port P_1 exists. Finally, the amplified SPPs couple to free-space modes. The surface plot corresponds to the z component of the magnetic field (A/m) at magnetic resonance. The middle part of the central superlattice, indicated by a box, is enlarged and the field amplitude is multiplied by 4 to clearly illustrate the mode profile.

which account for the external contribution of auxiliary ports P_3 and P_4 to the metamaterial ports P_1 and P_2. The primed parameters were found from the COMSOL simulation, and the unprimed parameters are the overall parameters corresponding to the two-port representation. The coefficient $\alpha/2$ is defined as the ratio of the optical power applied to each of the auxiliary ports P_3 and P_4 to the optical power applied to the input port P_1. The fields applied to the auxiliary ports P_3 and P_4 are always in phase and have equal power. Although the retrieval procedure assumes an infinite structure along the direction perpendicular to the direction of propagation of the incident field, we have verified that the retrieval procedure is applicable to finite-size ports (Fig. 1) excited by plane waves. This is similar to experimental characterization of finite metamaterial structures with finite beam spot size.

The commonly used FOM to quantify the loss compensation in NIMs is defined as $\mathrm{FOM} = -n'/n''$ [34,35,37], which is the same expression as the FOM used to measure the transparency of passive NIMs [15,63,64]. Although we can define the FOM for any arbitrary value of the refractive index, the FOM has a special importance when $n' = -1$ due to Pendry's perfect lens [2]. We denote this value of the FOM as FOM_{-1}. In order to maximize the FOM_{-1}, we need to aim for vanishing n'' while keeping $n' = -1$. This can be achieved by maximizing the amplitudes $|S'_{23}| = |S'_{24}| = |S'_{2a}|$ and removing the phase shift between S'_{23}, S'_{24}, and S'_{21} at the frequency where $n' = -1$, because the imaginary part of the refractive index n is responsible for the power loss in the structure and it can be minimized by increasing the transmittance while preserving the relation [34,38] $A + T + R = 1$ at the central superlattice. Here, absorbance $A = 1 - |S_{11}|^2 - |S_{21}|^2$, transmittance $T = |S_{21}|^2$, and reflectance $R = |S_{11}|^2$. Note that absorbance A of the central superlattice can be negative, hence implying gain.

The simplest design for the loss-compensated metamaterial can be obtained by using the same unit cell geometry of the original SPD NIM [49] for both the central superlattice and the symmetrically placed auxiliary superlattices with the exception that the gratings above the thin film in the auxiliary superlattices are removed to prevent the coupling of SPPs to free-space photons. Then, by tuning the α and the phase difference between the auxiliary ports and the input port P_1, n'' can be arbitrarily reduced at $n' = -1$, made zero, or even negative. The system does not become unstable and oscillatory when n'' becomes negative because the proposed scheme utilizes an open loop system that allows for only limited gain [65]. When $n'' = 0$ is reached at $n' = -1$, the frequency where this occurs may slightly shift [51]. If desired, this shift can be recalibrated through several iterations by slightly adjusting the system parameters. In this process, $|S'_{2a}|$ is preferred to be sufficiently large, since larger $|S'_{2a}|$ indicates larger plasmon injection rate, hence smaller required α (i.e., which means better performance). S'_{2a} can be tuned by changing the grating period and the distance between the side and central superlattices.

Below we use an optimized structure giving a maximum value of $|S'_{2a}|$ close to 0.2. The side superlattices of the structure have the grating period of 86 nm and are adjacent to the central superlattice. There exist six periods in each of the side superlattices and eight periods in the central superlattice. The phase shift between the auxiliary ports and the input port P_1 is almost zero.

In Fig. 2(a) we give the retrieved n' and n'' for the central superlattice for $\alpha = 6$. It is clearly seen that n'' is very close to zero in the negative index region implying low-loss operation. This is attributed to the compensation of the loss at the central superlattice by the SPPs excited through ports P_3 and P_4. Thus, the central superlattice forms our new low-loss NIM. We estimate the FOM_{-1} as 52, which is 21 times larger than the FOM_{-1} achieved by the same structure without the proposed loss compensation [49]. The result for retrieved impedance $z = z' + iz''$ is shown in Fig. 2(b). The

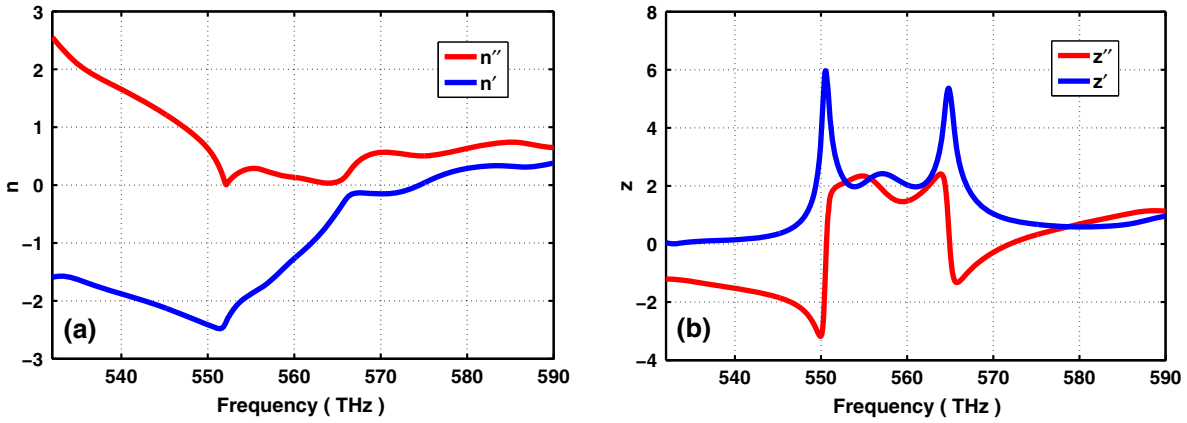

FIG. 2 (color online). Effective parameters for a single functional layer at $\alpha = 6$. (a) Real (n') and imaginary (n'') parts of the retrieved effective refractive index. Around 552 and 562 THz, the system behaves as an ultralow-loss NIM. (b) Real (z') and imaginary (z'') parts of the impedance.

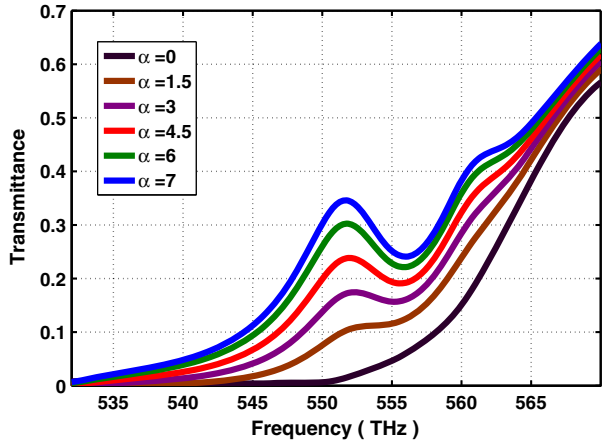

FIG. 3 (color online). Transmission spectra of the central superlattice. Transmittance through central superlattice increases with α. The increase in the transmittance is significant in the negative refractive index region around 560 THz.

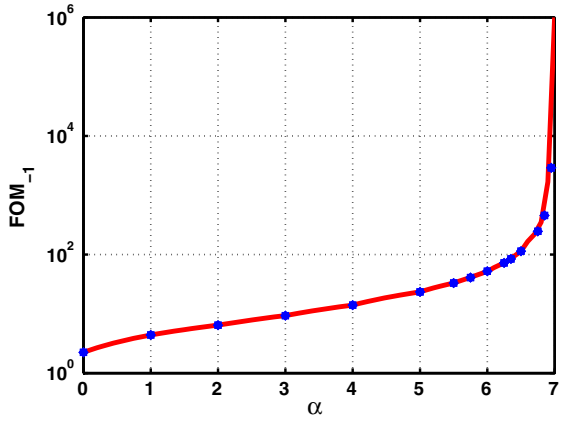

FIG. 4 (color online). The figure of merit for the negative index material (FOM_{-1}) as a function of α. The blue data points show the FOM_{-1} for the simulated values of α. The red solid line is the best-fit curve. FOM_{-1} diverges at $\alpha = 7$ and the metamaterial becomes loss free. Beyond $\alpha = 7$, the metamaterial becomes an amplifying medium.

features observed in the retrieved parameters are qualitatively similar to passive metamaterials including SPD NIMs [49], with the exception of relatively smoother variations, since such metamaterials are not as complex as the studied loss-compensated metamaterial structure, which involves, for example, finite-size effects and a plasmon injection rate varying with frequency [51]. A detailed discussion and subtle points behind the calculations of retrieved optical parameters in Fig. 2 are given in Ref. [51].

Figure 3 shows the overall transmittance $|S_{21}|^2$ through the central superlattice as a function of frequency for different values of α. Note that the transmittance increases with increasing α over most of the spectrum, including the negative index region at around 560 THz. These results depend on the amount of transferred power into the central superlattice and the phase necessary for the desired loss compensation but do not depend directly on the size of the auxiliary ports [51]. A detailed characterization of the device is given in Ref. [51]. We should note here that the output field at port P_2 is not just the simple summation of the output powers from individual sources (i.e., P_1, P_3, and P_4) but their coherent summation, which amplifies the signals due to constructive interference. Additional details on coherent loss-compensation and signal-amplification characteristics of the device based on phase-dependent transmittance are given in Ref. [51]. Additionally, there will be leakage to the output port from the auxiliary plasmonic fields even when the input P_1 is zero, but this is usually very low [51].

We have repeated the simulations for different values of the parameter α and calculated FOM_{-1}. The results are depicted in Fig. 4. FOM_{-1} rapidly increases with α and starts to diverge at a small value of $\alpha = 7$. The frequency corresponding to FOM_{-1} changes only slightly around 560 THz. In this regime, the medium becomes lossless (i.e., n'' approaches zero). Figure 4 shows that FOM_{-1} already becomes substantially large when α is between 6.5 and 7. Therefore, as long as α is tuned to this range, the resultant FOM_{-1} can be regarded as practically diverging, which means that the medium becomes practically loss free. This also makes the implementation experimentally feasible. Thus, the demonstrated rapid growth in FOM_{-1} shows that our loss-compensation scheme is a very effective solution to mitigate any type of losses (i.e., metallic, dielectric, and even losses due to fabrication imperfections) in metamaterials. Furthermore, the ultralow-loss bandwidth around the refractive index $n = -1$ can be also broadened [51].

Although the Drude model that we have used for gold underestimates the losses with respect to experimental values, this was chosen only for simplicity and does not invalidate the applicability of our loss-compensation scheme to highly lossy systems. Given the rapid growth in FOM_{-1} with increasing α as shown in Fig. 4 [51], the realistic experimental values for the permittivity of gold would only require larger α for loss-free operation, but not much larger than 7, because the metamaterial rapidly enters the amplifying regime beyond $\alpha = 7$.

The proof-of-principle plasmonic structures such as that given in Fig. 1 can be fabricated by self-aligned electron-beam lithography exposures and dielectric layer deposition via atomic layer deposition by choosing, for example, Ag as the metal and Al_2O_3 as the dielectric. Considering the experimental data [66] and misalignments, we have previously verified [67] that the negative index persists. We have confirmed through a series of sensitivity analyses that the structure is also tolerant to other imperfections possible at different stages of the fabrication process, including the variations in dielectric thickness (i.e., change from 8 to 15 nm), dielectric surface roughness (i.e., within $\pm 10\%$ of the average thickness), and strip width (i.e., $\pm 2.5\%$ change). Additional fabrication imperfections may further

deteriorate the negative index. However, we should note that as long as the underlying eigenmode (see the lower panel in Fig. 1) [51] of the metamaterial survives, the Π scheme cannot only restore the negative index but also makes the metamaterial loss free at only a larger α value than predicted theoretically. Similar metamaterial structures employing plasmonic modes, waveguide modes, or surface modes can also be designed and fabricated at lower frequencies with less difficulty. Loss-compensation schemes analogous to the Π scheme can be easily devised for other available metamaterials.

We should note that here we considered normal incidence only and accordingly designed the NIM structure. However, the underlying idea of plasmon injection for compensating and controlling losses can be generalized to an arbitrary form of incident waves. It is important to point out that the device does not have to know the form of incident waves, because the excitation of required eigenmodes, bulk and surface waves, amplitude, and phase relations can be automatically achieved [51]. The greatest challenge that hinders the advance of metamaterials and plasmonics, and prevents real-life applications in particular hyperlenses and superlenses, is the loss problem. Our loss-compensation scheme may revive these early dreams of metamaterials. For example, hyperlenses or superlenses with resolution significantly beyond the diffraction limit may be possible. Epsilon-near-zero materials [68] and transformation optics [6,7] can also benefit from this method. Our proposed scheme can also be applied to acoustic metamaterials to compensate damping in the same way as it is applied to electromagnetic waves here.

This work was supported by the National Science Foundation under Grant No. ECCS-1202443. We would like to thank Philip G. Evans at Oak Ridge National Laboratory for fruitful discussion on fabrication of proposed SPD plasmonic metamaterial structures, and Jae Yong Suh at Northwestern University for discussion on optical gain and amplification in plasmonic structures.

*Corresponding author.
dguney@mtu.edu

[1] V. G. Veselago, Sov. Phys. Usp. **10**, 509 (1968).
[2] J. B. Pendry, Phys. Rev. Lett. **85**, 3966 (2000).
[3] Z. Liu, H. Lee, Y. Xiong, C. Sun, and X. Zhang, Science **315**, 1686 (2007).
[4] X. Zhang and Z. Liu, Nat. Mater. **7**, 435 (2008).
[5] R. Junsuk, Z. Ye, Y. Xiong, X. Yin, Z. Liu, H. Choi, G. Bartal, and X. Zhang, Nat. Commun. **1**, 143 (2010).
[6] J. B. Pendry, D. Schurig, and D. R. Smith, Science **312**, 1780 (2006).
[7] U. Leonhardt, Science **312**, 1777 (2006).
[8] D. Schurig, J. J. Mock, B. J. Justice, S. A. Cummer, J. B. Pendry, A. F. Starr, and D. R. Smith, Science **314**, 977 (2006).
[9] N. I. Landy, S. Sajuyigbe, J. J. Mock, D. R. Smith, and W. J. Padilla, Phys. Rev. Lett. **100**, 207402 (2008).
[10] K. Aydin, V. E. Ferry, R. M. Briggs, and H. A. Atwater, Nat. Commun. **2**, 517 (2011).
[11] D. O. Guney and D. A. Meyer, Phys. Rev. A **79**, 063834 (2009).
[12] D. A. Genov, S. Zhang, and X. Zhang, Nat. Phys. **5**, 687 (2009).
[13] M. I. Aslam and D. O. Guney, Prog. Electromagn. Res. B **47**, 203 (2013).
[14] C. M. Soukoulis and M. Wegener, Science **330**, 1633 (2010).
[15] C. M. Soukoulis and M. Wegener, Nat. Photonics **5**, 523 (2011).
[16] D. O. Guney, T. Koschny, and C. M. Soukoulis, Phys. Rev. B **80**, 125129 (2009).
[17] D. O. Guney, T. Koschny, and C. M. Soukoulis, Opt. Express **18**, 12348 (2010).
[18] J. Gwamuri, D. O. Guney, and J. M. Pearce, *Solar Cell Nanotechnology*, edited by A. Tiwari, R. Boukherroub, and M. Sharon (Wiley, Hoboken, NJ, 2013), pp. 241–269.
[19] N. Papasimakis, V. A. Fedotov, N. I. Zheludev, and S. L. Prosvirnin, Phys. Rev. Lett. **101**, 253903 (2008).
[20] P. Tassin, L. Zhang, T. Koschny, E. N. Economou, and C. M. Soukoulis, Phys. Rev. Lett. **102**, 053901 (2009).
[21] J. Zhang, K. F. MacDonald, and N. I. Zheludev, Opt. Express **21**, 26721 (2013).
[22] G. V. Naik, J. Kim, and A. Boltasseva, Opt. Mater. Express **1**, 1090 (2011).
[23] G. V. Naik, J. L. Schroeder, X. Ni, A. V. Kildishev, T. D. Sands, and A. Boltasseva, Opt. Mater. Express **2**, 478 (2012).
[24] P. Tassin, T. Koschny, M. Kafesaki, and C. M. Soukoulis, Nat. Photonics **6**, 259 (2012).
[25] H. T. Chen, H. Yang, R. Singh, J. F. O'Hara, A. K. Azad, S. A. Trugman, Q. X. Jia, and A. J. Taylor, Phys. Rev. Lett. **105**, 247402 (2010).
[26] S. M. Anlage, J. Opt. **13**, 024001 (2011).
[27] C. Kurter, P. Tassin, A. P. Zhuravel, L. Zhang, T. Koschny, A. V. Ustinov, C. M. Soukoulis, and A. M. Anlage, Appl. Phys. Lett. **100**, 121906 (2012).
[28] A. L. Rakhmanov, A. M. Zagoskin, S. Savel'ev, and F. Nori, Phys. Rev. B **77**, 144507 (2008).
[29] A. L. Rakhmanov, V. A. Yampol'skii, J. A. Fan, F. Capasso, and F. Nori, Phys. Rev. B **81**, 075101 (2010).
[30] A. Shvetsov, A. M. Satanin, F. Nori, S. Savel'ev, and A. M. Zagoskin, Phys. Rev. B **87**, 235410 (2013).
[31] N. H. Shen, T. Koschny, M. Kafesaki, and C. M. Soukoulis, Phys. Rev. B **85**, 075120 (2012).
[32] N. P. Hylton, X. F. Li, V. Giannini, K. H. Lee, N. J. Ekins-Daukes, J. Loo, D. Vercruysse, P. Van Dorpe, H. Sodabanlu, M. Sugiyama, and S. A. Maier, Sci. Rep. **3**, 2874 (2013).
[33] E. Plum, V. A. Fedotov, P. Kuo, D. P. Tsai, and N. I. Zheludev, Opt. Express **17**, 8548 (2009).
[34] A. Fang, T. Koschny, and C. M. Soukoulis, Phys. Rev. B **82**, 121102(R) (2010).
[35] S. Wuestner, A. Pusch, K. L. Tsakmakidis, J. M. Hamm, and O. Hess, Phys. Rev. Lett. **105**, 127401 (2010).

[36] N. Meinzer, M. Ruther, S. Linden, C. M. Soukoulis, G. Khitrova, J. Hendrickson, J. D. Olitzky, H. M. Gibbs, and M. Wegener, Opt. Express **18**, 24140 (2010).
[37] S. Xiao, V. P. Drachev, A. V. Kildishev, X. Ni, U. K. Chettiar, H.-K. Yuan, and V. M. Shalaev, Nature (London) **466**, 735 (2010).
[38] A. Fang, Z. Huang, T. Koschny, and C. M. Soukoulis, Opt. Express **19**, 12688 (2011).
[39] S. Campione, M. Albani, and F. Capolino, Opt. Mater. Express **1**, 1077 (2011).
[40] I. Liberal, I. Ederra, R. Gonzalo, and R. W. Ziolkowski, Phys. Rev. Applied **1**, 044002 (2014).
[41] M. Infusino, A. D. Luca, A. Veltri, C. Vazquez-Vazquez, M. A. Correa-Duarte, R. Dhama, and G. Strangi, ACS Photonics **1**, 371 (2014).
[42] A. M. Keller, Y. Ghosh, M. S. DeVore, M. E. Phipps, M. H. Stewart, B. S. Wilson, D. S. Lidke, J. A. Hollingsworth, and J. H. Werner, Adv. Funct. Mater. **24**, 4796 (2014).
[43] D. Y. Fedyanin, A. V. Krasavin, A. V. Arsenin, and A. V. Zayats, Nano Lett. **12**, 2459 (2012).
[44] M. I. Stockman, Phys. Rev. Lett. **98**, 177404 (2007).
[45] P. Kinsler and M. W. McCall, Phys. Rev. Lett. **101**, 167401 (2008).
[46] J. A. Dionne, E. Verhagen, A. Polman, and H. A. Atwater, Opt. Express **16**, 19001 (2008).
[47] X. Chen, T. M. Grzegorczyk, B.-I. Wu, J. Pacheco, and J. A. Kong, Phys. Rev. E **70**, 016608 (2004).
[48] D. R. Smith, D. C. Vier, T. Koschny, and C. M. Soukoulis, Phys. Rev. E **71**, 036617 (2005).
[49] M. I. Aslam and D. O. Guney, Phys. Rev. B **84**, 195465 (2011).
[50] D. O. Guney, T. Koschny, and C. M. Soukoulis, Phys. Rev. B **83**, 045107 (2011).
[51] See Supplemental Material at http://link.aps.org/supplemental/10.1103/PhysRevLett.115.035502, which includes Refs. [2,17,34,35,37,47–50,52–59,62], for a detailed explanation of the working principle and general theory for the proposed loss-compensation scheme, the definitions of scattering parameters, the effect of α on the frequency where $n' = -1$, detailed device characterization, the calculation of retrieved optical parameters in Fig. 2, details on coherent compensation and amplification, the effect of loss compensation on n'' and FOM, the effect of α on the FOM, details on the eigenmode of the metamaterial, and the generalization of the Π scheme to a perfect lens.
[52] J. Zhou, Th. Koschny, M. Kafesaki, E. N. Economou, J. B. Pendry, and C. M. Soukoulis, Phys. Rev. Lett. **95**, 223902 (2005).
[53] C. E. Kriegler, M. S. Rill, S. Linden, and M. Wegener, IEEE J. Sel. Top. Quantum Electron. **16**, 367 (2010).
[54] C. A. Balanis, *Advanced Engineering Electromagnetics* (John Wiley and Sons, New York, 2012).
[55] Y. Cui, J. Xu, K. H. Fung, Y. Jin, A. Kumar, S. He, and N. X. Fang, Appl. Phys. Lett. **99**, 253101 (2011).
[56] C. Wu and G. Shvets, Opt. Lett. **37**, 308 (2012).
[57] A. Akyurtlu and A. G. Kussow, Phys. Rev. A **82**, 055802 (2010).
[58] S. Arslanagic, T. V. Hansen, N. A. Mortensen, A. H. Gregersen, O. Sigmund, R. W. Ziolkowski, and O. Breinbjerg, IEEE Antennas Propag. Mag. **55**, 91 (2013).
[59] J. Zhou, T. Koschny, M. Kafesaki, and C. M. Soukoulis, Phys. Rev. B **80**, 035109 (2009).
[60] D. O. Guney, T. Koschny, M. Kafesaki, and C. M. Soukoulis, Opt. Lett. **34**, 506 (2009).
[61] M. I. Aslam and D. O. Guney, J. Opt. Soc. Am. B **29**, 2839 (2012).
[62] S. Campione, S. Steshenko, M. Albani, and F. Capolino, Opt. Express **19**, 26027 (2011).
[63] J. Valentine, S Zhang, T. Zentgraf, E. Ulin-Avila, D. A. Genoc, G. Bartal, and X. Zhang, Nature (London) **455**, 376 (2008).
[64] C. Garcia-Meca, J. Hurtado, J. Marti, A. Martinez, W. Dickson, and A. V. Zayats, Phys. Rev. Lett. **106**, 067402 (2011).
[65] K. Ogata, *Modern Control Engineering* (Prentice-Hall, Englewood Cliffs, NJ, 2009).
[66] A. D. Rakic, A. B. Djurisic, J. M. Elazar, and M. L. Majewski, Appl. Opt. **37**, 5271 (1998).
[67] M. M. Rahman, M. I. Aslam, D. O. Guney, and P. G. Evans, in *Proceedings of the 7th International Congress on Advanced Electromagnetic Materials in Microwaves and Optics–Metamaterials* (IEEE, Bordeaux, 2013).
[68] X. Yang, C. Hu, H. Deng, D. Rosenmann, D. A. Czaplewski, and J. Gao, Opt. Express **21**, 23631 (2013).